BMP-7 attenuates left ventricular remodeling under pressure overload and facilitates reverse remodeling and functional recovery

David Merino1,2, Ana V. Villar1,2, Raquel García1,2, Mónica Tramullas1,2, Catalina Ribas4, Sofía Cabezudo4, J. Francisco Nistal2,3*, María A. Hurlé1,2,

1 Departamento de Fisiología y Farmacología, Facultad de Medicina, Universidad de Cantabria, Santander, Spain

2 Instituto de Investigación Marqués de Valdecilla (IDIVAL), Santander, Spain

3 Servicio de Cirugía Cardiovascular, Hospital Universitario Marqués de Valdecilla, Universidad de Cantabria, Santander, Spain

4 Departamento de Biología Molecular y Centro de Biologia Molecular "Severo Ochoa", CSIC-UAM, Universidad Autónoma de Madrid; Instituto de Investigación Sanitaria La Princesa, Madrid, Spain

*Corresponding authors:

J Francisco Nistal, Cirugía Cardiovascular, Hospital Universitario Marqués de Valdecilla, Avda. de Valdecilla 25, E-39008 Santander, Spain. Tel. (+34) 942 202 536, jfnistal@gmail.com

María A Hurlé, Departamento de Fisiología y Farmacología, Facultad de Medicina, Universidad de Cantabria, Avda. Herrera Oria s/n, E-39011 Santander, Spain. Tel. (+34) 942 201 981 hurlem@unican.es

Abstract

Transforming Growth Factors (TGF)-β regulate tissue fibrosis: TGF-β promotes fibrosis, whereas Bone Morphogenetic Protein (BMP)-7 is antifibrotic. **Aims**: To demonstrate that: (i) Left ventricular (LV) remodeling after pressure overload is associated to disequilibrium in the signaling mediated by these cytokines; and (ii) BMP-7 exerts beneficial effects on LV remodeling and reverse remodeling. **Methods and Results**: We studied patients with aortic stenosis (AS) and mice subjected to transverse aortic constriction (TAC) and TAC-release (de-TAC). LV morphology and function were assessed by echocardiography. LV biopsies were analyzed by qPCR, immunoblotting and histology. Pressure overload reduced BMP-7 and pSmad1/5/8 and increased TGF-β and pSmad2/3 in AS-patients and TAC-mice. BMP-7 correlated inversely with collagen, fibronectin and β-MHC expressions, and with hypertrophy and diastolic dysfunction, and directly with the systolic function. Multiple linear regression disclosed BMP-7 and TGF-β as hypertrophy predictors, negative and positive, respectively. BMP-7 prevented TGF-β-elicited hypertrophic program in cardiomyocytes, and Col1A1 promoter activity in NIH-3T3 fibroblasts. The treatment of TAC-mice

with rBMP-7 attenuated the development of structural damage and dysfunction, and halted ongoing remodeling. The reverse remodeling after pressure overload release was facilitated by rBMP-7, and hampered by disrupting BMP-7 function using a neutralizing antibody or genetic deletion. Conclusion: The disequilibrium between BMP-7 and TGF-β signals plays a relevant role in the LV remodeling response to hemodynamic stress in TAC-mice and AS-patients. BMP-7 signaling protects the LV against pathological remodeling and might constitute a therapeutic target to delay or avoid surgery, and to improve the reverse remodeling after surgery in AS patients.

Key words: Aortic stenosis, pressure overload, myocardial remodeling, BMP-7, TGF-β

Abbreviations

AS: Aortic stenosis

BMP: Bone Morphogenetic Protein

E/e′: ratio of peak early transmitral flow velocity (E) to peak early myocardial tissue velocity (e′)

ECM: Extracellular matrix

EMT: Endothelial-to-mesenchymal transition

LV: Left ventricle

LVEDd: LV end diastolic diameter

LVEF: LV ejection fraction

LVESd: LV end systolic diameter

MAPSE: mitral annular plane systolic excursion

PO: Pressure overload

PWT: LV Posterior wall thicknesses

PWT/LVEDr: Relative PWT to LVED radius

TAC: Transverse aortic constriction

TGF-β Transforming Growth Factor

Introduction

Aortic stenosis (AS) is an age-related valve disorder; it constitutes the most common adult heart valve disease that requires surgery in the Western world and it will keep gaining importance due to the progressive increase in life expectancy in our societies [1]. Sustained pressure overload (PO) stress can elicit in the LV from AS patients a harmful remodeling, characterized by concentric hypertrophy and interstitial and perivascular fibrosis [2], which constitutes a major independent risk factor for heart failure and mortality [3]. Nowadays, the only effective therapy for symptomatic AS patients is the aortic valve replacement. After releasing the biomechanical stress, the LV undergoes a process of reverse remodeling [4,5]. However, when the LV structural damage is severe the remodeling process becomes irreversible after surgery, which results in unfavorable short- and long-term outcome of AS patients [4,6,7]. The lack of preventive therapies of myocardial remodeling in AS patients highlights need for new effective drugs to delay the progression of LV structural damage before surgery and to improve and accelerate the reverse remodeling after releasing the hemodynamic stress.

The transforming growth factor β (TGF-βs) superfamily of cytokines is composed, among others, by the prototypic TGF-βs and bone morphogenetic proteins (BMPs). TGF-β and BMP signaling [8] is transmitted by heteromeric complexes of type I (also termed activin like kinase [ALK]) and type II membrane receptors, with serine/threonine kinase activity. Upon receptor activation, the canonical intracellular signals propagate downstream through the phosphorylation of receptor-activated Smads; p-Smads form complexes with the common partner, Smad4, which translocate to the nucleus to regulate the transcription of target genes. The TGF-β subfamily signals through pSmad2/3, while the BMP family signals through pSmad1/5/8 proteins. These signals can be controlled by negative-feedback mechanisms via inhibitory Smads [9,10].

Overproduction of TGF-β contributes to cardiomyocyte hypertrophy and aberrant synthesis and deposition of extracellular matrix (ECM) which characterizes the pathological remodeling of the LV under PO in animal models and in patients suffering from AS or systemic hypertension [11-17]. TGF-βs promote resident fibroblast proliferation and activation, and stimulate endothelial-to-mesenchymal transition (EMT), increasing the pool of cardiac myofibroblasts [11,14]. On the other hand, BMP-7 signaling counteracts TGF-β1-induced accumulation of myofibroblasts and extracellular matrix (ECM) production in experimental models of progressive interstitial fibrosis affecting several organs, including the heart [18,19]. In the present study we investigated the pathophysiological relevance of an imbalance between TGF-β and BMP-7 signaling in the LV remodeling response to PO in patients suffering of severe AS and in a mouse model of transverse aortic constriction (TAC). The potential for BMP-7 to prevent, slow, or reverse the LV structural damage induced by PO, and to improve the LV reverse remodeling after releasing the hemodynamic stress was assessed in mice.

Methods

Pressure overload studies in mice.

The experiments were performed in 12-16 week old littermate female wild type (C57BL/6) and heterozygous BMP-7 deficient mice (BMP-$7^{+/-}$) in a C57BL/6 genetic background [20]. The study was approved by the University of Cantabria Institutional Laboratory Animal Care and Use Committee (reference IP0415) and conducted in accordance with the guidelines from directive 2010/63/EU of the European Parliament. All animals received humane care and all efforts were made to minimize animal suffering.

Transverse aortic constriction (TAC) and release (de-TAC): Mice were anesthetized by intraperitoneal injection of ketamine (100 mg/kg) and xylazine (5 mg/kg) and subjected to transverse aortic constriction (TAC) for 4 weeks [16]. In a series of mice, the aortic arch was re-approached and the constriction was released (de-TAC mice); de-TACmice were followed-up for one or four weeks. Mice were sacrificed by decapitation under anesthesia (100 mg/kg ketamine and 5 mg/kg xylazine, i.p.).

Treatments: the protocols and number of mice per group are shown in the supplementary Fig S1. Recombinant murine BMP-7 (rBMP-7, R&D Systems) was administered at the dose of 10 µg/kg/week using osmotic mini-pumps (Alzet 1002) during: (i) the complete 4 week-TAC period; (ii) the 3rd and 4th weeks following TAC; or (iii) the first week after de-TAC. A monoclonal anti-BMP-7 antibody (clone 164313, R&D Systems) was administered daily (12 µg/day, i.p.) for 7 days starting at the de-TAC surgery.

Echocardiography: Transthoracic echocardiography was performed with ultrasound equipment [Vevo-770 (VisualSonics, Toronto, ON, Canada) using a high-resolution transducer centered at 30 MHz]. The operator was blinded to the study groups. Transcoarctational pressure gradients were measured using pulsed wave Doppler analysis at the distal arch. LV end-diastolic (LVEDd) and end-systolic (LVESd) internal diameters, interventricular septum (IVST) and LV posterior wall (PWT) thicknesses were measured following the recommendations of the American Society of Echocardiography. The degree of geometric concentricity of the remodeled LV was assessed by the relative PWT (rPWT) calculated as: rPWT=PWT/(LVEDd/2). Cardiac mass was estimated using the Devereux's formula. The mitral annular plane systolic excursion (MAPSE) measurements were obtained from four-chamber views using M-mode imaging. The LV ejection fraction (LVEF) and MAPSE were used as surrogates of short axis and longitudinal systolic functions, respectively. Parameters of diastolic LV function (E/e') were obtained by pulsed-wave mitral inflow analysis and tissue Doppler imaging to obtain the ratio of peak early transmitral flow velocity (E) to peak early myocardial tissue velocity (e′).

Pressure overload studies in patients

The study followed the Declaration of Helsinki guidelines for biomedical research involving human subjects. The institutional ethics and clinical research committee approved the study and all patients gave written informed consent. The clinical and demographic characteristics of the AS and control groups are shown in Supplementary Table S1. The study was performed using LV myocardial intraoperative biopsies obtained from a cohort of 37 patients diagnosed with isolated severe AS and undergoing aortic valve replacement

surgery in the University Hospital Marqués de Valdecilla in Santander, Spain. Patients with aortic or mitral regurgitation greater than mild or with major coronary stenosis greater than 50%, previous cardiac operations, malignancies or poor renal or hepatic function were deemed ineligible for the study. The control group was a cohort of 32 surgical patients with pathologies (atrial septal defect: n=18, aortic aneurysm: n=7, mitral stenosis: n=4, left atrial myxoma: n=2, pulmonary valve fibroelastoma: n=1) that did not associate LV pressure or volume overload, coronary heart disease or cardiomyopathies. Subepicardial biopsies (4 to 10 mg) were taken from the LV lateral wall with a Tru-cut needle during the surgical procedure.

Studies in cultured cells

Rat neonatal cardiomyocytes: Cardiomyocytes were obtained from Wistar rats sacrificed by decapitation at postnatal day 2–3. The hearts were removed and kept in Ca^{2+}/Mg^{2+}-free HBBS (Hank´s Balanced Salt Solution) medium at 4ºC. The tissues were minced using a sterile scalpel blade and transferred to a T25 flask containing trypsin (1x, Sigma), type IV collagenase (200 U/ml, Sigma), type I collagenase (0,025 mg/ml, Sigma) and DNase I (0,2 U/ml, Sigma). The flask was settled at 37ºC for 15min and the supernatant was then collected, mixed with HBBS medium and centrifuged (5min, 1500 rpm). The cell pellet was re-suspended in DMEM supplemented with 5% FBS and kept at 37ºC. The harvested cells were plated and incubated for 2 h to allow the attachment and removal of fibroblasts. The cardiomyocytes were plated (300,000 cells per well) in M12 multi-well plates pre-coated with 1% gelatin and cultured in DMEM supplemented with 10%FBS for 48h. The culture medium was then replaced with OPTI-MEM containing TGF-β1 (5 nmol/ml), BMP-7 (20 nmo/ml) or TGF-β1 (5 nmol/ml) plus BMP-7 (20 nmo/ml) and incubated for 24 h. The cells were collected and processed for mRNA isolation. Five independent experiments were performed.

NIH-3T3 fibroblasts and dual luciferase reporter assays: NIH-3T3 fibroblasts (ATCC, USA) were cultured in DMEM supplemented with 10% FBS, 100 U/ml penicillin-streptomycin, at 37°C in 5% CO_2. The cells were seeded in 96 well plates ($2x10^4$/well) and cultured for 24 hours in opti-MEM medium. The cells were co-transfected with pGL3-reporter luciferase vector containing the promoter of Col1A1 (100 ng/well). The DNA transfection reagent was X-tremeGENE 9 (Roche Diagnostics, Germany). The cells were incubated for 24 h with OPTI-MEM containing TGF-β1 (5 nmol/ml), BMP-7 (20 nmo/ml) or TGF-β1 (5 nmol/ml) plus BMP-7 (20 nmo/ml). Luciferase activity was assessed using a Luciferase® Reporter Assay (Promega) according to the manufacturer's specifications. The assays were performed in three wells on two separate experiments.

mRNA expression

Total RNA was obtained by TRIzol (Invitrogen) extraction. Real-time q-PCR was conducted using specific TaqMan assays (Applied Biosystems) for the following genes: BMP-7, TGF-β1, TGF-β2, Smad2, Smad3, Smad7, collagen I (Col1A1), collagen III (Col3A3), fibronectin 1 (FN1), β-myosin heavy chain (β-MHC), atrial natriuretic peptide (ANP) and brain natriuretic peptide (BNP). Gene expression levels were normalized to ribosomal 18S RNA.

Duplicate transcript levels were determined in a minimum of three independent experiments.

Histology

Hearts were fixed in paraformaldehyde (3.7% in PBS) for 48 h and included in paraffin. Four short axis sections (5 µm) at the level of the papillary muscles (n=4 mice per experimental condition) were stained using Masson's trichrome. Digital photographs of the full LV sections were captured using a camera (Axiocam MRc5, Zeiss) attached to a stereo-microscope (Zeiss Axiomat). The fractional area of fibrosis was determined (ImageJ software) and the results were expressed as the blue-stained areas divided by the total LV myocardial area. The minor diameters of cardiomyocytes from the subendocardial region of the posterior wall were measured (25 cells per field, 3 fields per mice and 4 mice per group). The operator was blinded to the experimental group.

Western Blot

Thirty µg of protein lysates were electrophoresed on 10% sodium dodecyl sulfate-polyacrylamide gel and transferred onto polyvinylidene difluoride membranes (Bio-Rad, California, USA). The primary antibodies were: Goat polyclonal to p-Smad2/3 (Santa Cruz Biotechnology, sc-11769), rabbit poyclonal to p-Smad1/5/8 (cell signaling 9511S); rabbit monoclonal to Smad7 (Abcam, ab90086); mouse monoclonal to BMP7 (R&D, MAB71405); mouse monoclonal to GAPDH (Santa Cruz, sc-32233); and mouse monclonal to Tubulin (Sigma-Aldrich, T5168). After incubation with the appropriate secondary antibodies, proteins were immunodetected with ECL Advance Western Blotting Detection Kit (GE Healthcare) or with infrared fluorescence (Odyssey imager). The results were expressed as optical density of the sample dots normalized to that obtained for GAPDH or tubulin. Samples from 3-6 subjects per group were tested in two independent experiments.

Statistics

Data were assessed for normality with the Kolmogorov-Smirnov test. Values were reported as means ± S.E.M. Continuous variables were compared using two-tailed Student's t-test or Mann-Whitney U test. The influence of genotype, drug treatments and PO on gene expression was assessed by a two-way ANOVA, and, on echocardiographic parameters by repeated-measures two-way ANOVA. Bonferroni post hoc test was used when appropriate. Correlations between mRNA expression levels were performed using Pearson's correlation analysis. Multiple linear regression analysis was used to identify predictors of LV hypertrophy. Post-hoc assessment of the regression model in patients was performed with the bootstrapping method with 2,000 iterations. Significance levels: *p<0.05, **p<0.01, ***p<0.001. Statistical packages: GraphPad Prism 5.03 and PASW Statistics 18 (SPSS Inc., Chicago, IL).

Results

LV remodeling involves unbalance between TGF-β1- and BMP-7-mediated signaling in a mouse model of pressure overload.

TAC caused a stable trans-coarctational pressure gradient of ≈50 mmHg during the 4 week follow-up period (Fig 1A). PO resulted in the development of a rapid progressive LV hypertrophy with concentric geometry (increased LVPWT/LVEDr), which was accompanied by LV systolic functional deterioration both in the radial (LVEF) and longitudinal axes (MAPSE), and diastolic dysfunction reflected by the rise in the LV filling pressure (E/e′). Four weeks after TAC, mice were subjected to de-TAC surgery and the morpho-functional echocardiographic evolution was followed for 4 further weeks (Fig 1A). The release of overload stress activated the reverse remodeling process; as a result, LV mass decreased and LVEF, MAPSE and E/e′ improved significantly within the first week after de-TAC. Then, recovery continued at a more gradual rhythm and at 4 weeks, even though LVEF and E/e′ had already normalized their values, LV mass and MAPSE had not yet returned to baseline figures (Fig 1A).

LV expression of BMP-7 mRNA (Fig 1B) was significantly reduced in mice subjected to TAC, whereas the transcript levels of TGF-β1 and TGF-β2 underwent up-regulation; consequently, the ratios TGF-βs/BMP-7 increased significantly. The mRNA levels of the inhibitory Smad7 were significantly reduced (Fig 1B). Protein levels of p-Smad2/3 increased while those of p-Smad1/5 and Smad7 diminished (Fig 1C).

Four weeks after releasing the overload stress, the expression levels of BMP-7, the ratios TGF-β1/2 to BMP-7, and the expressions of p-Smad2/3, p-Smad1/5/8 and Smad7 recovered the control values (Figs 1B and C).

Lineal regression analysis, performed in the cohorts of TAC and de-TAC mice, show that BMP-7 in the LV correlated significantly and inversely with the mRNA levels of TGF-β1 and TGF-β2, and directly with those of the inhibitory Smad7 (Fig 2A). Additionally, the transcript levels of BMP-7 correlated significantly and inversely with the expression of genes encoding extracellular matrix elements (Col1A1, Col3A3 and FN-1) (Fig 2B), consistent with the antifibrogenic properties of this cytokine.

Both, the sarcomeric hypertrophic marker β-MHC (Fig 2B) and LV mass correlated negatively with BMP-7 (Fig 2C), suggesting an anti-hypertrophy role for BMP-7. Thus, multiple regression analysis (Fig 2D) indicated that the myocardial expression of BMP-7 constituted an independent negative predictor of LV posterior wall thickening after TAC, whereas TGF-β2 was a positive predictor. The regression equation was the following: PWT (mm) = 0.73 - 1.45*[BMP-7] + 0.2*[TGF-β2]. The adjusted R^2 (0.53; $p<0.001$) indicates that 53% of the variance in PWT after TAC can be estimated from this model.

Regarding the echocardiographic functional parameters, BMP-7 transcript levels correlated inversely with the mean trans-coarctation gradient in TAC mice (R = 0.52**), indicating a relationship between the severity of the constriction and BMP-7 down-regulation. Moreover, the systolic function was positively related to myocardial BMP-7, both in the short-axis (LVEF) and in the long-axis (MAPSE); while the degree of diastolic dysfunction, as reflected by the increase in E/e′, was inversely related to BMP-7 mRNA levels (Fig 2C).

BMP-7 inhibits TGF-β-induced hypertrophic program in primary cultures of cardiomyocytes

In cultured neonatal rat ventricular cardiomyocytes, the addition of recombinant BMP-7 (20 ng/ml) to the culture medium reduced significantly the overexpression of the hypertrophy markers, ANP, BNP and β-MHC, induced by TGF-β (3 ng/ml) (Fig 3A).

BMP-7 prevents TGF-β-induced transcriptional activation of the Col1A1 promoter in NIH-3T3 fibroblasts.

The stimulation with TGF-β1 (3 ng/ml) of NIH-3T3 fibroblasts, transfected with a full-length promoter of COL1A1-Luc construct, resulted in significant increase of the luciferase activity. BMP-7 (20 ng/ml) significantly repressed transcriptional activation of COL1A1Pro-luc by TGF-β1 (3 ng/ml) (Fig 3B).

Sustained treatment with recombinant BMP-7 protects the LV from remodeling under biomechanical stress

The usefulness of rmBMP-7 as pre-emptive treatment against LV remodeling and to stop the ongoing pathological remodeling response was assessed under the following experimental conditions (Fig S1): (i) mice treated with a 4-week subcutaneous infusion of rmBMP-7 starting at the moment of TAC surgery (BMP-$7^{1\text{-}4wk}$ group); (ii) mice treated with a 2-week subcutaneous infusion rmBMP-7 starting on day 15 after TAC surgery when LV hypertrophy and functional deterioration were already taking place (BMP-$7^{3\text{-}4wk}$ group); and (iii) TAC mice treated with a 4-week subcutaneous infusion of saline as control group.

TAC caused similar trans-coarctation pressure gradients (Fig 4A) in saline and rmBMP-7 treated mice at any time of the follow-up, indicating similar degrees of constriction in all groups. The administration of rmBMP-7 during the 4 week TAC follow-up period diminished PO-induced PW and IVS thickening as well as chamber dilation; as a result, BMP-$7^{1\text{-}4wk}$ mice developed a significantly lower degree of LV hypertrophy as compared with saline treated mice. BMP-7 completely prevented TAC-induced systolic dysfunction in the short-axis (LVEF), and the LV systolic function in the long-axis (MAPSE) was significantly less impaired in BMP-$7^{1\text{-}4wk}$ than in the saline group. The rise in E/e' induced by TAC was completely prevented by BMP-$7^{1\text{-}4wk}$, which indicates a protection against the development of diastolic dysfunction (Fig 4A).

The treatment with rmBMP-7 during the complete TAC period prevented myocardial overexpression of the remodeling-related genes analyzed (TGF-β1, TGF-β2, Col1A1, Col3A3, FN1 and β-MHC) (Figs 5A-F), and attenuated the structural remodeling, as indicated milder histological fibrosis and shorter cardiomyocyte diameters displayed by BMP-$7^{1\text{-}4wk}$ compared with saline treated mice (Figs 5G-I) .

The administration of rmBMP-7 during the 3rd and 4th weeks of TAC halted the progression of wall thickening, LV hypertrophy, chamber dilation and systolic and diastolic dysfunctions (Fig 4A). The expressions of the remodeling-related genes were lower in BMP-$7^{3\text{-}4wk}$ than in TAC mice treated with saline (Figs 5A-F). At the structural level, the average cardiomyocyte diameter (Fig 5I) was significantly smaller, and the LV area occupied by histological fibrosis (Figs 5G and H) displayed a decremental trend, but without statistical significance due to the interindividual variability.

Overall, our results indicate that down-regulation of BMP-7 during the hemodynamic stress condition was a relevant maladaptive feature of myocardial remodeling and that sustained administration of recombinant BMP-7 prevented PO-induced myocardial hypertrophy, structural damage and systolic and diastolic dysfunctions. Moreover, when treatment begins once the pathological myocardial remodeling has been established, BMP-7 can stop the progression of the ongoing structural damage and its deleterious functional consequences.

BMP-7 deficiency potentiates LV hypertrophy in BMP-7$^{+/-}$ mice under biomechanical stress

BMP-7$^{+/-}$ mice exhibited at baseline significantly larger thicknesses of LV walls and LV mass than their WT littermates. No differences between genotypes were evidenced in chamber dimensions, systolic and diastolic functions. Following TAC, the two genotypes developed similar transcoarctational gradients (wild type: 46.1±3.1 mmHg; BMP-7$^{+/-}$: 45.6±2.5 mmHg). However, BMP-7$^{+/-}$ mice developed greater levels of LV hypertrophy and a more concentric LV geometry than wild type mice. The systolic (LVEF and MAPSE) and diastolic (E/e′) functions displayed a similar deterioration in both genotypes at any time after TAC (Fig 4B). At the structural level (Fig 6B), the average diameter of cardiomyocytes was larger in BMP-7$^{+/-}$ than in their wild type littermates both at baseline and after TAC. The degree of myocardial fibrosis developed was higher in BMP-7$^{+/-}$ than in C57BL/6 mice.

LV reverse remodeling in mice is hampered by BMP-7 signaling loss-of-function and improved by recombinant BMP-7

Four weeks after TAC a series of mice were subjected to de-TAC surgery. Given that the bulk of the remodeling regression had occurred within the first week after de-TAC (Fig 1A), the follow-up of this part of the study was limited to one week after de-TAC surgery. We assessed the influence of BMP-7 signaling loss-of-function on the capability of the heart to reverse the LV remodeling after PO release by de-TAC surgery (Fig 6). The subjects of study (see Fig S1) were the following: (i) TAC-BMP-7$^{+/-}$ mice treated with a subcutaneous saline infusion during 7 days after de-TAC; (ii) TAC-WT mice treated with daily injections of a specific monoclonal neutralizing antibody against BMP-7 (BMP-7-Ab, 500 µg/kg/day, 7 days) starting at the moment of de-TAC surgery; and (iii) TAC-WT mice treated with a subcutaneous saline infusion during 7 days after de-TAC.

The transcoarctational gradient fell significantly after de-TAC surgery with no differences between groups (de-TAC+saline: 16.9±2.3; de-TAC BMP-7$^{+/-}$ +saline: 12.5±1.2; de-TAC+BMP-7-Ab: 17.6±1.1). Both, heterozygous deletion of BMP-7 and BMP-7 neutralization with a BMP-7-Ab during the 7 day de-TAC period hampered the LV morpho-functional recovery after releasing the hemodynamic stress. Regression of LV hypertrophy and the recovery of systolic (LVEF and MAPSE) and diastolic (E/e′) functions were significantly worse in both groups of loss-of-BMP-7 function in comparison with C57BL/6 mice treated with saline (Fig 6A). At the structural level (Fig 6B), the remaining fibrosis and the average cardiomyocyte diameter after 1-wk de-TAC were significantly

higher in BMP-$7^{+/-}$ mice and in mice treated with BMP-7-Ab than in wild type littermates treated with saline.

The effect of BMP-7 gain-of-function on reverse remodeling was assessed in a series of wild type mice treated with rmBMP-7 during the 7-day de-TAC period (Fig 6A). The loss of LV mass during the first de-TAC week was significantly higher in rmBMP-7-treated than in saline-treated mice. Chamber dilation (LVEDd and LVESd; not shown) decreased and systolic function (LVEF and MAPSE) improved to a significantly greater extents with rmBMP-7 than with saline treatment during the first week after de-TAC. At the structural level (Fig 6B), both saline- and rmBMP-7-treated mice reduced the cardiomyocyte diameter and LV fibrosis area to similar extents.

Translation of the results obtained in the experimental model to the clinical aortic stenosis

The LV myocardium from AS patients exhibited significantly lower BMP-7 and higher TGF-β1 preoperative expression levels compared with surgical controls (Fig 7A). BMP-7 mRNA levels in the AS patients' heart correlated significantly and inversely with the gene expression of TGF-β1 and directly with SMAD7 (Fig 7B). As observed in TAC mice, the myocardial gene expression of BMP-7 correlated inversely with the expressions of Col1A1 and Col3A3 (Fig 7B), and there was a significant and positive association between BMP-7 expression and the systolic function in the short axis (LVEF). Consistent with an antihypertrophic effect induced by BMP-7, there was an inverse and significant relationship between the cytokine and the LV mass (Fig 7B). Stepwise multiple linear regression analysis (Fig 7C) evidenced that preoperative BMP-7 was a significant negative predictor of the LV mass, whereas TGF-β1 appeared as a significant positive predictor. The regression equation was the following: LV mass (g) = 257.5 - 111.6*[BMP-7] + 21.3*[TGF-β1]. The adjusted R^2 (0.45; $p<0.001$) indicated that 45% of the variance in LV mass can be estimated from this model in AS patients.

Discussion

Our findings in patients with severe AS and in a mouse model of reversible pressure overload raise two important notions: (i) an imbalance between BMP-7 and TGF-β signals could play a major etiopathogenic role in the maladaptive LV remodeling under pressure overload; and (ii) strategies to enhance the activity of BMP-7 signaling may have putative therapeutic value to attenuate ongoing myocardial hypertrophy and to favor the reverse remodeling after releasing the LV from the hemodynamic load.

TGF-β and BMP-7 belong to the same superfamily, however, each of these cytokines exhibit a unique signaling pathway through specific Smad proteins that determine some effects that are opposite in each pathway [8,18,19]. During the process of pathological remodeling induced by hemodynamic stress, TGF-β is a primary and potent mediator of myocardial fibrosis and hypertrophy both in mice and humans [11-17]. On the other hand, BMP-7 acts as an anti-fibrotic cytokine in experimental models of pathological organ fibrosis [18,19,21-26]. Our current results evidenced that pressure overload resulted in biased cellular signaling towards pro-fibrogenic cytokines of the TGF-β family in detriment of BMP-7-mediated signals, both in TAC mice and

in AS patients. We observed LV up-regulation of TGF-βs and down-regulation of BMP-7 expressions and increased TGF-βs/BMP-7 ratio. Accordingly, the levels of BMP-7 canonical down-stream effectors (pSmads1/5/8) were reduced while those of TGF-β (pSmad2/3) appeared increased. In the group of pressure-overloaded mice, the balance between TGF-βs and BMP-7 signaling recovered normal values after releasing the hemodynamic stress by de-TAC. Furthermore, myocardial mRNA levels of BMP-7 and those of TGF-βs correlated inversely both in the cohort of operated mice and in AS patients. These results support the existence of a reciprocal inhibition between BMP-7 and TGF-β in the heart, and suggest its clinical relevance in human cardiac remodeling diseases.

TGF-β signaling is modulated by inhibitory Smads. Smad7 binds TGF-β type I receptor and inhibits Smad2/3 phosphorylation [8,9]. Down-regulation of Smad7 has been reported to potentiate TGF-β-mediated post-infarct fibrosis in rats [27]; conversely, recombinant Smad7 protects against angiotensin II-induced hypertensive cardiac remodeling in mice [28]. Our present results show that Smad7 was down-regulated in the LV from TAC mice and AS patients, which suggest its contribution to the strengthened TGF-β biased fibrotic signaling. In cultured cells, BMP-7 induces Smad7 transcription by interacting with BMP responsive elements in the promoter [29]; therefore, BMP-7 down-regulation in the pressure overload condition could release TGF-β signaling from the Smad7 antagonistic activity.

BMP-7 prevents and even reverses, *in vitro*, TGF-β-induced EMT, fibroblast accumulation and transdifferentiation into myofibroblasts, blocks the production of ECM proteins by these cells, and stimulates MMP-2-dependent breakdown of the fibrotic matrix [18,19,30-32]. Our findings in vivo show that the transcript levels of BMP-7 kept an inverse relationship with the expression of Col1A1, Col3A3 and FN1 in the LV from TAC mice. Moreover, the luciferase-reporter assays indicate that BMP-7 inhibits Col1A1 promoter transcription activity induced by TGF-β in cultured NIH-3T3 fibroblasts. Interstitial fibrosis is a major cause of LV wall stiffening, diastolic and systolic dysfunction and progression to heart failure [2,33]. Accordingly, BMP-7 expression in TAC-mice was related directly to parameters of systolic function (LVEF and MAPSE), and inversely to the degree of diastolic dysfunction, reflected by the LV filling pressure (E/e′).

LV hypertrophy, although long considered beneficial to preserve fiber shortening in the afterload excess condition [3], is now recognized as an independent predictor of cardiovascular events as well as of global and cardiovascular mortality [34-36]. Persistence of LV hypertrophy after aortic valve replacement in AS patients stands as a limiting factor for short and long-term outcome [4-7], whereas LV mass normalization constitutes an independent positive predictor of long-term survival in multivariate analysis [37]. BMP-7 has been reported to be involved in cardiac myogenesis in the chick embryo [38], and BMP type I and type II receptors and signaling pathways are functional in cardiac myocytes from humans, mice and rats [39]. However, to our knowledge, there are no studies addressing a possible role for BMP-7 in the regulation of cardiomyocyte function and pathophysiology. Our data strongly suggest that BMP-7 exerts an antihypertrophic effect. Such statement is based upon the following findings: (i) In TAC-mice, there was an inverse relationship between

BMP-7 gene expression and LV mass, which is concordant with the negative correlation between the expressions of BMP-7 and the hypertrophy marker, β-MHC. (ii) The treatment with recombinant BMP-7 after TAC attenuated significantly the degree of LV hypertrophy developed. (iii) BMP-$7^{+/-}$ mice, compared to wild type, exhibited a higher LV wall thickness and LV mass at baseline and, under PO, and developed a greater degree of LV hypertrophy with more concentric geometry. (iv) Regression of LV hypertrophy after de-TAC was improved by recombinant BMP-7 while it was hampered by BMP-7 loss-of function. (v) Multiple regression analysis in TAC mice showed that myocardial transcript levels of BMP-7 and TGF-β2 constituted significant independent predictors, negative and positive respectively, which can explain as much as 53% of the variance in PW thickness after 4 weeks of TAC. (vi) rmBMP-7 inhibited the capability of TGF-β to activate in vitro the cardiomyocyte "hypertrophic gene program," of which ANP, BNP and β-MHC are prototypical members [40].

Most of the results obtained in the experimental model can be translated into a prevalent clinical condition of PO such as aortic valve stenosis. Thus, the LV from severe AS patients exhibited a lower BMP-7 expression and a higher TGF-β/BMP-7 ratio compared with surgical controls and both transcripts correlated inversely. As observed in TAC-mice, BMP-7 mRNA expression levels in the LV from AS patients correlated inversely with those of Col1A1 and collagen III as well as with the systolic function in the short axis (LVEF). Also, multiple regression analysis in AS patients showed that myocardial transcript levels of BMP-7 and TGF-β1 constituted significant independent predictors, negative and positive respectively, of the LV mass variance (46%).

Overall, our findings strongly suggest that, during the myocardial remodeling process in mice and patients, lower myocardial expression levels of BMP-7 associate higher TGF-β signaling, more severe structural damage and stronger functional echocardiographic abnormalities. Interestingly, a previous report on patients with type 2 diabetes mellitus shows that the circulating levels of BMP-7 and TGF-β1 are better predictors (negative and positive, respectively) of the future decline in kidney function than conventional markers [41].

In line with a protective effect against pathological remodeling, the treatment of TAC-mice with exogenous rmBMP-7 during the complete follow-up period after TAC prevented the development of myocardial fibrosis and, as a result, the systolic (LVEF and MAPSE) and diastolic (E/e′) functional deteriorations were significantly attenuated when compared with saline treated TAC-mice. From a clinical point of view, a major finding of our study is that BMP-7 not only prevented LV remodeling, but also halted its progression when the treatment started on day 14th after TAC, when LV hypertrophy and functional deterioration were already taking place. In these animals, the progression of the LV hypertrophy and chamber dilation ceased, the overexpression of ECM-related genes and histological fibrosis tapered and there was a tendency to improve the systolic function, in both the radial (FEVI) and longitudinal (MAPSE) axes, as well as the diastolic function. Furthermore, BMP-7 signaling also seems to play a relevant positive role in the reverse remodeling process after releasing PO, as evidenced our pharmacological and genetic approaches. Both, the treatment of mice with a BMP-7 neutralizing

antibody, and BMP-7 haploinsufficiency hampered significantly the ability of the LV to recover the normal myocardial structure and function after de-TAC. On the contrary, exogenously administered rmBMP-7 improved some features of the reverse remodeling; particularly hypertrophy, chamber dilation and radial systolic function were significantly improved during the de-TAC recovery period by this treatment.

The putative benefit of the activation of BMP-7 signaling to resolve established organ damage has been investigated in rodent models of renal, hepatic and pulmonary progressive fibrosis [21-26]. Of note, small peptide agonists of the ALK3 type of BMP-7 receptors have been generated to inhibit kidney inflammation, tissue damage and fibrosis [25], and one such peptide, THR–184, is currently being evaluated in clinical studies of renal injury (NIH, ClinicalTrials.gov Identifier: NCT01830920).

In summary, our findings support that the imbalance between BMP-7 and TGF-β opposing signals may play an important role in the remodeling response of the heart to the hemodynamic stress. The results strongly suggest that BMP-7 signaling might constitute a new therapeutic target for the palliative treatment of AS patients with severe, although asymptomatic, LV remodeling in order to delay or even avoid surgery. Additionally, the improvement by pharmacologic means of LV reverse remodeling after valve replacement could have positive consequences in the short- and long-term survival and clinical status of these patients.

Acknowledgements: We acknowledge the technical assistance of Amalia Cavayé (HUMV), Ana Cayón (IDIVAL), Nieves García (UC), Elena Martín (RN, HUMV), Roberto Moreta (RN, HUMV) and María Navarro (IDIVAL). BMP-$7^{+/-}$ mice were kindly provided by Dr Elizabeth J. Robertson, Department of Molecular and Cellular Biology, Harvard University, Cambridge, MA 02138, USA.

Financial support: This work was supported by grants from the Ministerio de Economía y Competitividad [Fondo de Investigaciones Sanitarias (PI12/00999, PI14/00201 and PI15/01224), Red de Investigación Cardiovascular [(RD12/0042/0018 and RD12/0042/0012), and Plan Estatal de Investigación Científica, Técnica y de Innovación (SAF2013-47434-Retos)] and from the Fundación Ramón Areces. Co-funded by the Fondo Europeo de Desarrollo Regional (FEDER).

Disclosures: None

References

1. Iung B, Baron G, Tornos P, Gohlke-Bärwolf C, Butchart EG, Vahanian A. Valvular heart disease in the community: a European experience.Curr Probl Cardiol. 2007; 32:609-661.
2. Burchfield JS, Xie M, Hill JA. Pathological ventricular remodeling: mechanisms: part 1 of 2. Circulation. 2013; 128(4):388-400.
3. Grossman W, Paulus WJ. Myocardial stress and hypertrophy: a complex interface between biophysics and cardiac remodeling. J Clin Invest. 2013; 123:3701-3703.
4. Lund O, Emmertsen K, Dørup I, Jensen FT, Flø C. Regression of left ventricular hypertrophy during 10 years after valve replacement for aortic stenosis is related to the preoperative risk profile. Eur Heart J. 2003; 24:1437-1446.
5. Villar AV, Merino D, Wenner M, Llano M, Cobo M, Montalvo C, García R, Martín-Durán R, Hurlé JM, Hurlé MA, Nistal JF. Myocardial gene expression of microRNA-133a and myosin heavy and light chains, in conjunction with clinical parameters, predict regression of left ventricular hypertrophy after valve replacement in patients with aortic stenosis. Heart. 2011; 97:1132-1137.
6. Krayenbuehl HP, Hess OM, Monrad ES, Schneider J, Mall G, Turina M.

   Left ventricular myocardial structure in aortic valve disease before, intermediate, and late after aortic valve replacement. Circulation. 1989; 79:744-755.
7. Weidemann F, Herrmann S, Störk S, Niemann M, Frantz S, Lange V, Beer M, Gattenlöhner S, Voelker W, Ertl G, Strotmann JM. Impact of myocardial fibrosis in patients with symptomatic severe aortic stenosis. Circulation. 2009; 120:577-584.
8. Massagué J. TGFβ signalling in context. Nat Rev Mol Cell Biol. 2012; 13:616-630.
9. Yan X, Chen YG. Smad7: not only a regulator, but also a cross-talk mediator of TGF-β signalling. Biochem J. 2011; 434:1-10.
10. Dooley S, Hamzavi J, Ciuclan L, Godoy P, Ilkavets I, Ehnert S, Ueberham E, Gebhardt R, Kanzler S, Geier A, Breitkopf K, Weng H, Mertens PR. Hepatocyte-specific Smad7 expression attenuates TGF-beta-mediated fibrogenesis and protects against liver damage. Gastroenterology. 2008; 135:642-659.
11. Zeisberg EM, Tarnavski O, Zeisberg M, Dorfman AL, McMullen JR, Gustafsson E, Chandraker A, Yuan X, Pu WT, Roberts AB, Neilson EG, Sayegh MH, Izumo S, Kalluri R. Endothelial-to-mesenchymal transition contributes to cardiac fibrosis. Nat Med. 2007; 13:952–961.
12. Villar AV, Cobo M, Llano M, Montalvo C, González-Vílchez F, Martín-Durán R, Hurlé MA, Nistal JF. Plasma levels of transforming growth

factor-beta1 reflect left ventricular remodeling in aortic stenosis. PLoS One. 2009; 4(12):e8476

13. Dobaczewski M, Chen W, Frangogiannis NG. Transforming growth factor (TGF)-β signaling in cardiac remodeling. J Mol Cell Cardiol. 2011; 51:600-606.

14. Koitabashi N, Danner T, Zaiman AL, Pinto YM, Rowell J, Mankowski J, Zhang D, Nakamura T, Takimoto E, Kass DA. Pivotal role of cardiomyocyte TGF-β signaling in the murine pathological response to sustained pressure overload. J Clin Invest. 2011; 121:2301-2312.

15. Montalvo C, Villar AV, Merino D, García R, Ares M, Llano M, Cobo M, Hurlé MA, Nistal JF. Androgens contribute to sex differences in myocardial remodeling under pressure overload by a mechanism involving TGF-β. PLoS One. 2012; 7(4):e35635.

16. Villar AV, García R, Llano M, Cobo M, Merino D, Lantero A, Tramullas M, Hurlé JM, Hurlé MA, Nistal JF. BAMBI (BMP and activin membrane-bound inhibitor) protects the murine heart from pressure-overload biomechanical stress by restraining TGF-β signaling. Biochim Biophys Acta Mol Basis Dis. 2013; 1832:323-335.

17. Beaumont J, López B, Hermida N, Schroen B, San José G, Heymans S, Valencia F, Gómez-Doblas JJ, De Teresa E, Díez J, González A. microRNA-122 down-regulation may play a role in severe myocardial fibrosis in human aortic stenosis through TGF-β1 up-regulation. Clin Sci (Lond). 2014; 126:497-506.

18. Zeisberg M, Hanai J, Sugimoto H, Mammoto T, Charytan D, Strutz F, Kalluri R. BMP-7 counteracts TGF-beta1-induced epithelial-to-mesenchymal transition and reverses chronic renal injury. Nat Med. 2003; 9:964-968.

19. Weiskirchen R, Meurer SK. BMP-7 counteracting TGF-beta1 activities in organ fibrosis. Front Biosci. 2013; 18:1407-1434.

20. Godin RE, Takaesu NT, Robertson EJ, Dudley AT. Regulation of BMP7 expression during kidney development. Development. 1998; 125:3473-3482.

21. Morrissey J, Hruska K, Guo G, Wang S, Chen Q, Klahr S. Bone morphogenetic protein-7 improves renal fibrosis and accelerates the return of renal function. J Am Soc Nephrol. 2002; 13:S14-21.

22. Wang S, de Caestecker M, Kopp J, Mitu G, Lapage J, Hirschberg R. Renal bone morphogenetic protein-7 protects against diabetic nephropathy. J Am Soc Nephrol. 2006; 17:2504-2512.

23. Kinoshita K, Iimuro Y, Otogawa K, Saika S, Inagaki Y, Nakajima Y, Kawada N, Fujimoto J, Friedman SL, Ikeda K. Adenovirus-mediated expression of BMP-7 suppresses the development of liver fibrosis in rats. Gut. 2007; 56:706-714.

24. Sugimoto H, Yang C, LeBleu VS, Soubasakos MA, Giraldo M, Zeisberg M, Kalluri R. BMP-7 functions as a novel hormone to facilitate liver regeneration. FASEB J. 2007; 21:256-2 64.

25. Sugimoto H, LeBleu VS, Bosukonda D, Keck P, Taduri G, Bechtel W, Okada H, Carlson W Jr, Bey P, Rusckowski M, Tampe B, Tampe D, Kanasaki K, Zeisberg M, Kalluri R. Activin-like kinase 3 is important for kidney regeneration and reversal of fibrosis. Nat Med. 2012; 18:396-404.

26. Urbina P, Singla DK. BMP-7 attenuates adverse cardiac remodeling mediated through M2 macrophages in prediabetic cardiomyopathy. Am J Physiol Heart Circ Physiol. 2014; 307:H762-772.

27. Wang B, Hao J, Jones SC, Yee MS, Roth JC, Dixon IM. Decreased Smad 7 expression contributes to cardiac fibrosis in the infarcted rat heart. Am J Physiol Heart Circ Physiol. 2002; 282:H1685-1696.

28. Wei LH, Huang XR, Zhang Y, Li YQ, Chen HY, Yan BP, Yu CM, Lan HY. Smad7 inhibits angiotensin II-induced hypertensive cardiac remodelling. Cardiovasc Res. 2013; 99:665-673.

29. Benchabane H, Wrana JL. GATA- and Smad1-dependent enhancers in the Smad7 gene differentially interpret bone morphogenetic protein concentrations. Mol Cell Biol. 2003; 23:6646-6661.

30. Pegorier S, Campbell GA, Kay AB, Lloyd CM. Bone morphogenetic protein (BMP)-4 and BMP-7 regulate differentially transforming growth factor (TGF)-beta1 in normal human lung fibroblasts (NHLF). Respir Res. 2010; 11:85.

31. Wang S, Hirschberg R. Bone morphogenetic protein-7 signals opposing transforming growth factor beta in mesangial cells. J Biol Chem. 2004; 279:23200-23206.

32. Midgley AC, Duggal L, Jenkins R, Hascall V, Steadman R, Phillips AO, Meran S. Hyaluronan regulates Bone Morphogenetic Protein-7 dependent prevention and reversal of myofibroblast phenotype. J Biol Chem. 2015 Feb 25.

33. Cohn JN, Ferrari R, Sharpe NR. Cardiac remodeling-concepts and clinical implications: a consensus paper from an international forum on cardiac remodeling. Behalf of an International Forum on Cardiac Remodeling. J Am Coll Cardiol. 2000; 35:569-582.

34. Levy D, Garrison RJ, Savage DD, Kannel WB, Castelli WP. Prognostic implications of echocardiographically determined left ventricular mass in the Framingham Heart Study. N Engl J Med. 1990; 322:1561-1566.

35. Lorell BH, Carabello BA. Left ventricular hypertrophy: pathogenesis, detection, and prognosis. Circulation. 2000;102:470-479.

36. Berenji K, Drazner MH, Rothermel BA, Hill JA. Does load-induced ventricular hypertrophy progress to systolic heart failure? Am. J. Physiol. Heart Circ. Physiol. 2005; 289:H8-H16.

37. Ali A, Patel A, Ali Z, Abu-Omar Y, Saeed A, Athanasiou T, Pepper J. Enhanced left ventricular mass regression after aortic valve replacement in patients with aortic stenosis is associated with improved long-term survival. J Thorac Cardiovasc Surg. 2011; 142:285-291.

38. Schultheiss TM, Burch JB, Lassar AB. A role for bone morphogenetic proteins in the induction of cardiac myogenesis. Genes Dev. 1997; 11:451-462.

39. Wu X, Sagave J, Rutkovskiy A, Haugen F, Baysa A, Nygård S, Czibik G, Dahl CP, Gullestad L, Vaage J, Valen G. Expression of bone morphogenetic protein 4 and its receptors in the remodeling heart. Life Sci. 2014; 97:145-154.

40. Dorn GW 2nd, Robbins J, Sugden PH Phenotyping hypertrophy: eschew obfuscation. Circ Res. 2003; 92:1171-1175.

41. Wong MG, Perkovic V, Woodward M, Chalmers J, Li Q, Hillis GS, Yaghobian Azari D, Jun M, Poulter N, Hamet P, Williams B, Neal B, Mancia G, Cooper M, Pollock CA. Circulating bone morphogenetic protein-7 and transforming growth factor-β1 are better predictors of renal end points in patients with type 2 diabetes mellitus. Kidney Int. 2013; 83:278-84.

Legends

Figure 1. **A**: Echocardiographic morphological and functional changes induced by pressure overload in mice subjected to 4 week transverse aortic constriction (TAC, n=17), and their recovery 4 week after releasing the aortic constriction (de-TAC, n=8). Data are expressed as mean ± SEM Repeated-measures ANOVA followed by Bonferroni's test. **B**: Myocardial mRNA levels of BMP-7, TGF-β1 and TGF-β2 and the ratios between TGFβs and BMP7 in sham, TAC and de-TAC mice. ANOVA followed by Bonferroni's test (sham, n=7; TAC, n=8; de-TAC, n=7). **C**: Myocardial levels of Smads in sham (n=4), TAC (n=5) and de-TAC (n=4) mice. pSmad1/5/8 and pSmad2/3 were determined by western blot. The optical density was normalized to tubulin or GAPDH and expressed as percentage of change vs sham mice. Smad7 was determined by qPCR (sham, n=6; TAC, n=6; de-TAC, n=7) and western blot (n=4 mice per group). Representative western blots belong to the same gel. ANOVA followed by Bonferroni's test (see supplementary statistical analysis). RE: Relative mRNA expression normalized to 18S.

Figure 2. Linear regression and Pearson′s correlation analyses showing the relationship of BMP-7 mRNA expression with elements of TGF-β signaling (**A**), remodeling-related genes (**B**), and morpho-functional echocardiographic parameters (**C**) in the LV myocardium from TAC (n=7-17 mice) and de-TAC-mice (n=7). R: Pearson′s correlation coefficient. **D**: Multiple linear regression model for predicting the posterior wall thickness after 4 weeks of TAC (n=17). Adjusted R^2=0.53 ($p<0.001$). RE: Relative mRNA expression normalized to 18S.

Figure 3. The effects of BMP-7 on TGF-β-induced hypertrophic program in cultured cardiomyocytes **(A** to **C)**. Relative mRNA expression (RE vs18S) of the hypertrophy markers ANP, BNP and β-MHC were determined by q-PCR in five independent experiments. **D**: Effect of recombinant BMP-7 on TGF-β1-induced luciferase activity in NIH-3T3 cells transfected with the promoter region of Col1A1 in a luciferase reporter vector. Cells were treated with TGF-β1 (5 nmol/ml), BMP-7 (20 nmo/ml) or TGF-β1 (5 nmol/ml) plus BMP-7 (20 nmo/ml). The luciferase assay was performed in three wells on two separate experiments. ANOVA followed by Bonferroni's test (see supplementary statistical analysis).

Figure 4. A: Echocardiographic morpho-functional changes induced by pressure overload in TAC-mice. PWT: LV Posterior wall thicknesses; LVESd: LV end systolic diameter; LVEDd: LV end diastolic diameter; PWT/LVEDr: Relative PWT to LVED radius; LVEF: LV ejection fraction; MAPSE: mitral annular plane systolic excursion; E/e′: ratio of peak early transmitral flow velocity (E) to peak early myocardial tissue velocity (e′). Data are expressed as mean ± SEM. **A:** Mice were treated with saline (n=8, open circles), rBMP7 during the 4 week TAC period (n=5, black circles) or rBMP7 during the 3rd and 4th weeks after TAC (n=8, black squares). Two way repeated-measures ANOVA

followed by Bonferroni's test (*TAC-saline vs. TAC-BMP-$7^{1\text{-}4wk}$; $^{\#}$TAC-saline vs. TAC-BMP-$7^{3\text{-}4wk}$). **B**: Wild type (n=8, open circles) and BMP-$7^{+/-}$ mice (n=15, black circles) follow-up. (See supplementary statistical analysis).

Figure 5. Myocardial mRNA expression levels of TGF-βs (**A**: TGF-β1 and **B**: TGF-β2), fibrosis markers (**C**: Col I, **D**: Col III and **E**: FN-1) and hypertrophy marker (**F**: β-MHC) in sham (n=6-12), TAC-saline (n=8-11), TAC-BMP-$7^{1\text{-}4wk}$ (n=5) and TAC-BMP-$7^{3\text{-}4wk}$ (n=6) mice. **G**: Representative images of Masson trichrome–stained LV sections showing myocardial fibrosis in blue. The percentage of the LV area occupied by fibrosis (**H**) and the average diameter of cardiomyocytes (**I**) were determined in 4 LV sections from 3-6 mice per group. ANOVA followed by Bonferroni's test (see supplementary statistical analysis).

Figure 6. Effects of BMP7 loss- and gain-of function on the reverse remodeling during the first week after de-TAC. In a series of mice, four weeks after TAC the aortic constriction was removed (de-TAC) and mice were followed-up for one week after de-TAC. C57BL6 mice were treated with saline (n=8), a BMP7 neutralizing antibody (n=6, BMP7-Ab) or recombinant BMP7 (n=5). BMP$7^{+/-}$ mice were treated with saline after de-TAC (n=7). **A**: LV hypertrophy regression after de-TAC. Recovery of systolic function in the short axis (LVEF). **C**: Recovery of systolic function in the long axis (MAPSE). Reduction of LV loading pressure (E/e'). Data are expressed as mean ± SEM of the percentage of change vs 4 wk-TAC. **B**: The percentage of fibrosis and the cardiomyocyte diameter were measured in LV sections from 3-6 mice per group stained with Masson trichrome. Data are means ± SEM. ANOVA followed by Bonferroni's test (see supplementary statistical analysis).

Figure 7. A: Myocardial expression of BMP-7, TGF-β1 and Smad7 in the LV from AS (n=38) and surgical control patients (n=32) determined by qPCR and western blot (n=3-4 patients per group). In each representative western blot, the dots belong to the same gel. Mann Witney U test. **B**: Linear regression and Pearson′s correlation analyses showing the relationship of BMP-7 mRNA levels with TGF-β1, Smad7, collagens I and III, LV mass index (LVMI) and LV ejection fraction (LVEF). R: Pearson′s correlation coefficient. **C**: Significant preoperative predictors of LV mass in AS patients undergoing aortic valve replacement (n=38). Adjusted R^2=0.53 ($p<0.001$). RE: Relative expression normalized to the ribosomal subunit 18S.

Figure 1

Click here to download Figure(s): BMP7 FINAL Fig 1 version 2 cardiovasc res.tif

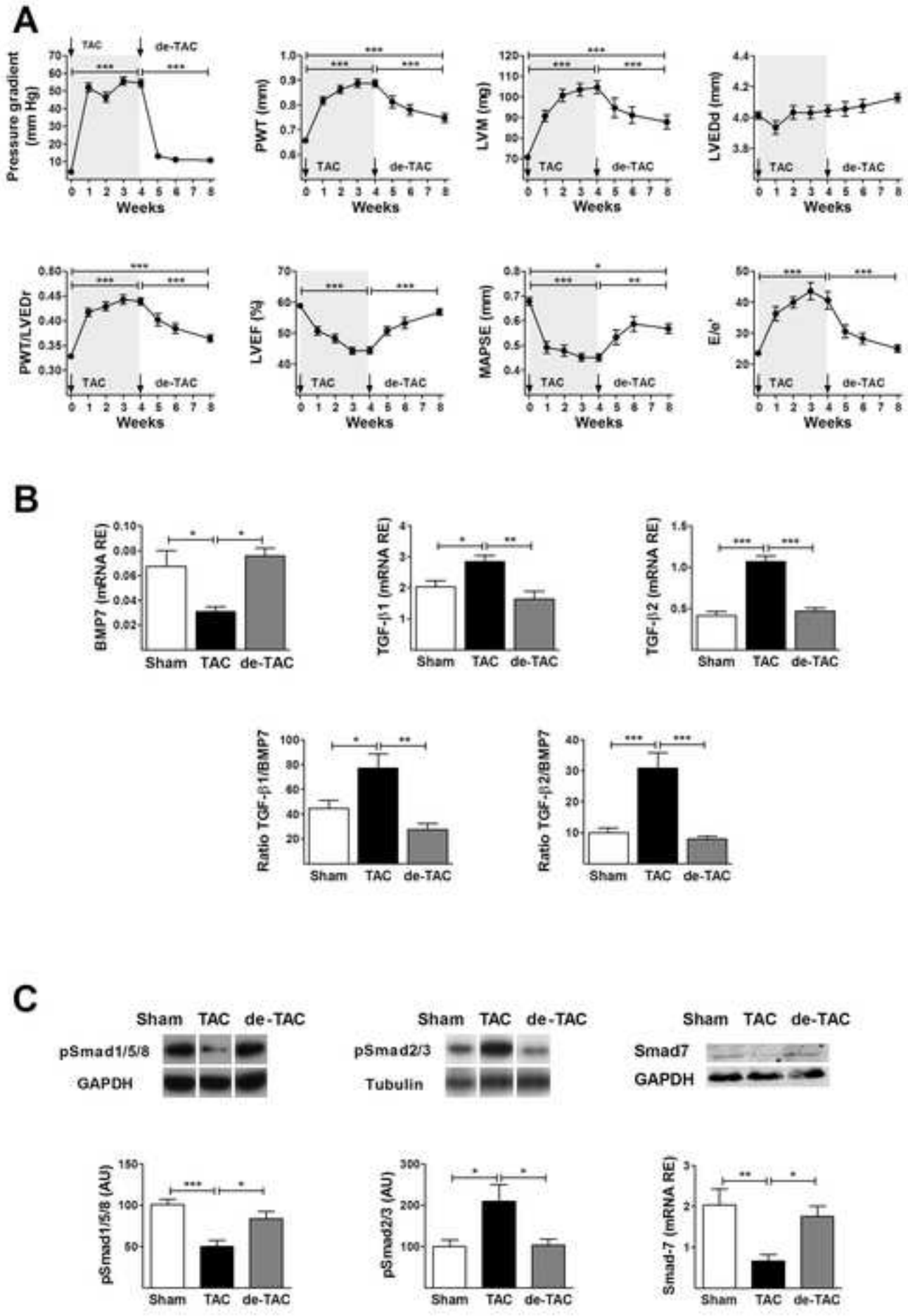

Figure 2

Click here to download Figure(s): BMP7 Fig 2 cardiovasc res.tif

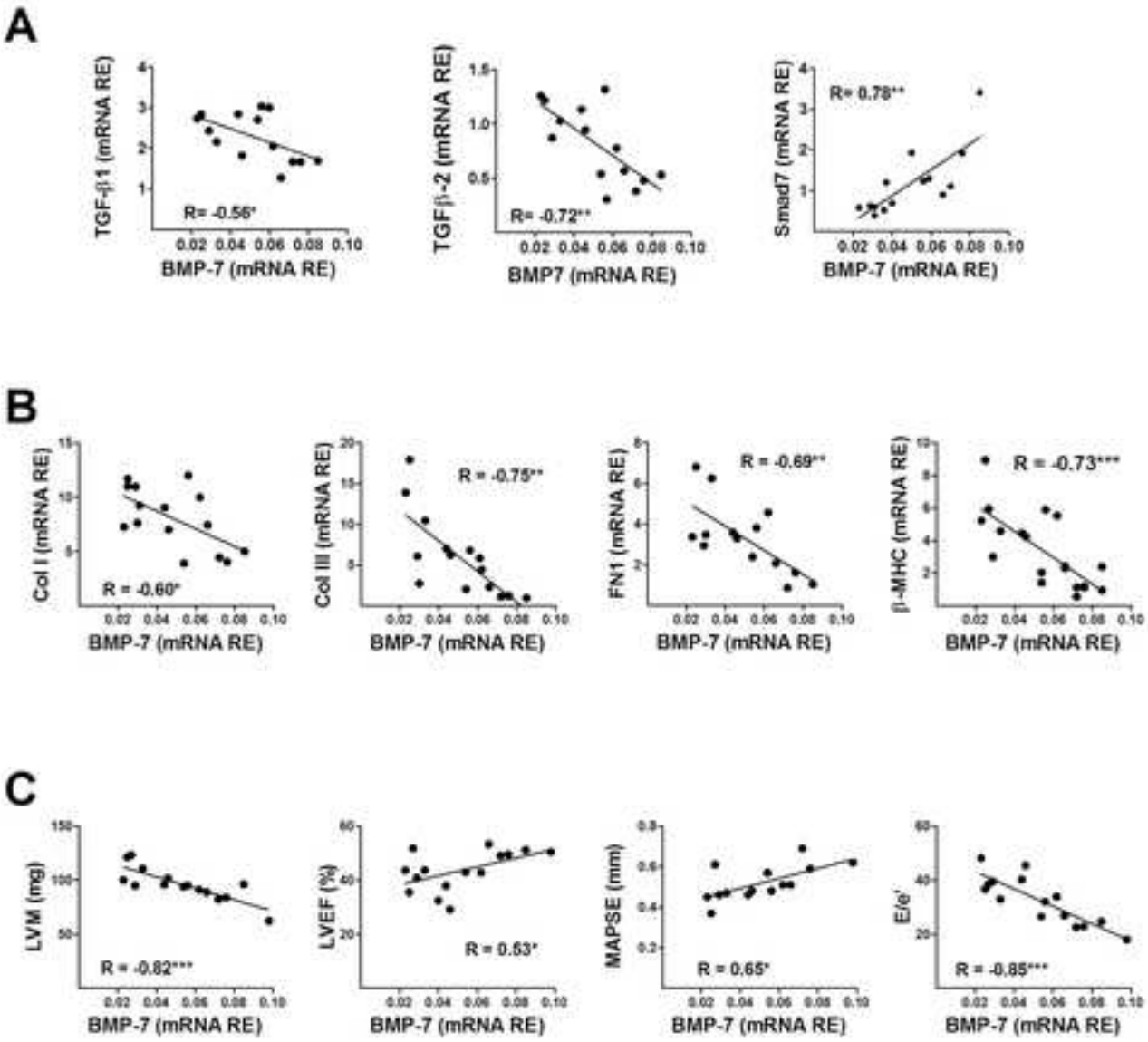

D

Predictors of posterior wall thickness (mm) in TAC mice *(Multiple linear regression analysis)*				
Variable	**Unstandardized Coefficient**		**Standardized Coefficient β**	**p value**
	B	**Std. Error**		
Myocardial BMP-7 (RE *vs* 18S)	-1,451	0.68	-0.35	0.05
Myocardial TGF-β2 (RE *vs* 18S)	0.2	0.05	0.61	0.002

Figure 3
Click here to download Figure(s): BMP7 Fig 3 cardiovasc res.jpg

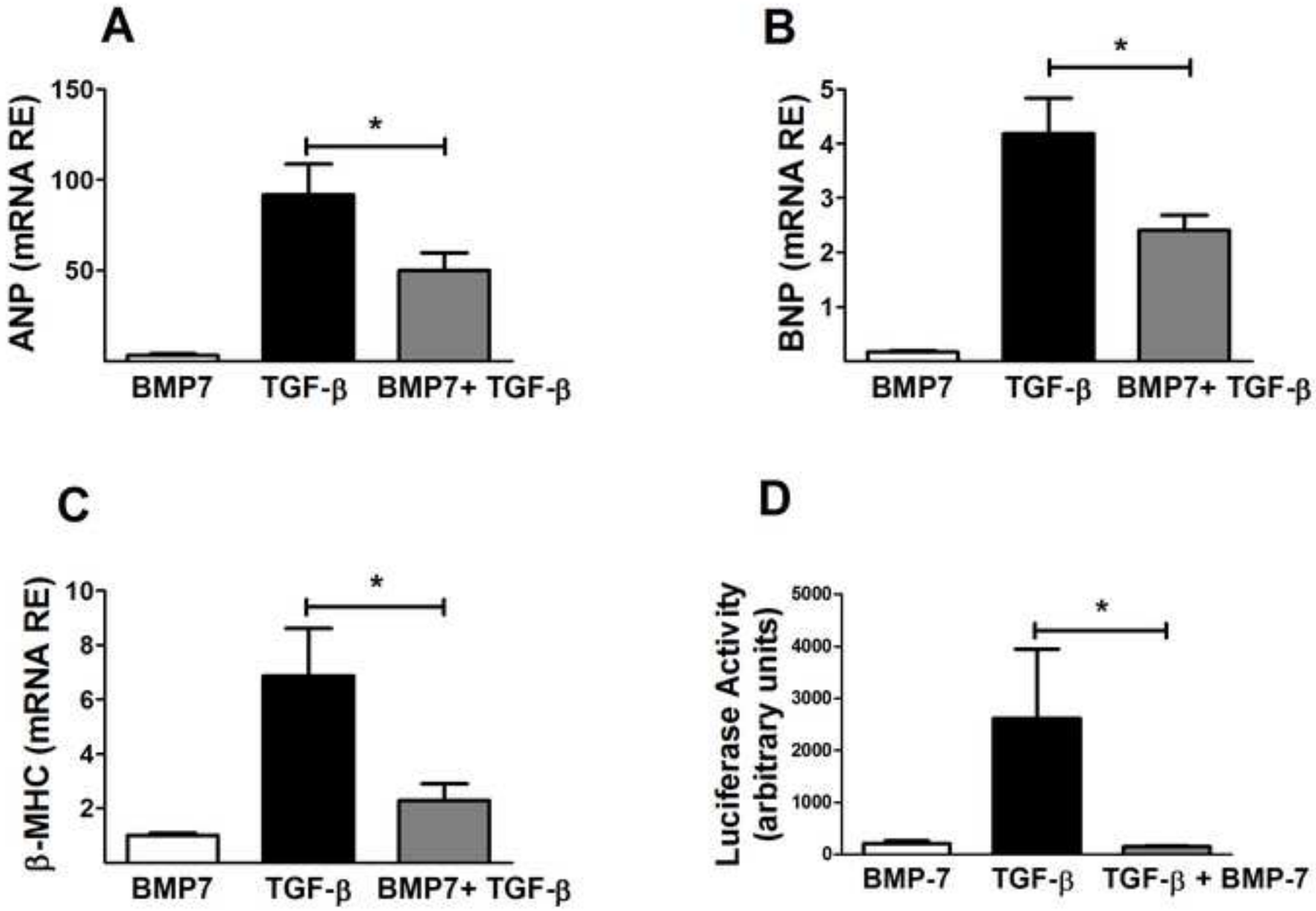

Figure 4

Click here to download Figure(s): BMP7 Fig 4 Ay B final.tif

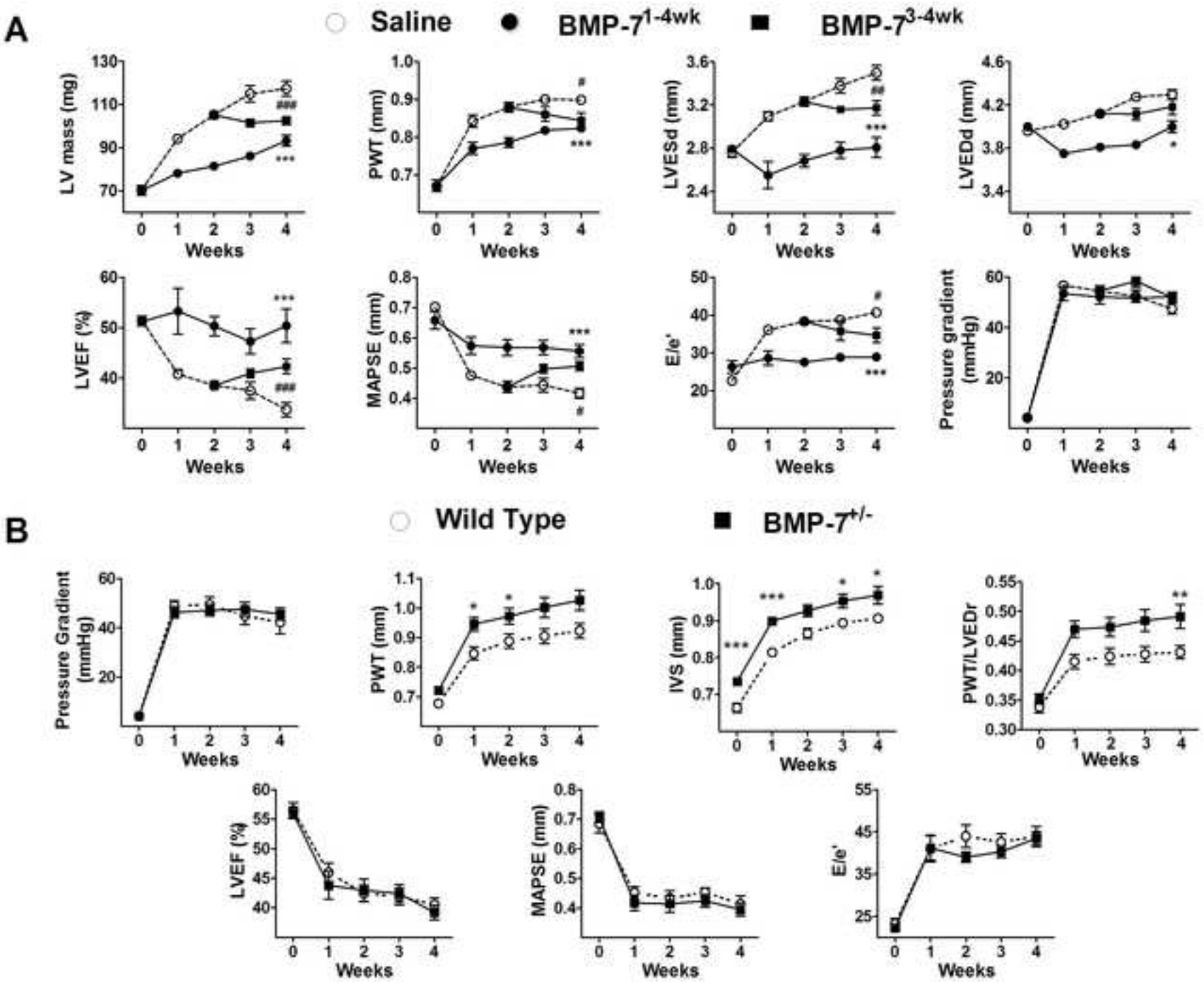

Figure 5

Click here to download Figure(s): BMP7 Fig 5 cardiovasc res.jpg

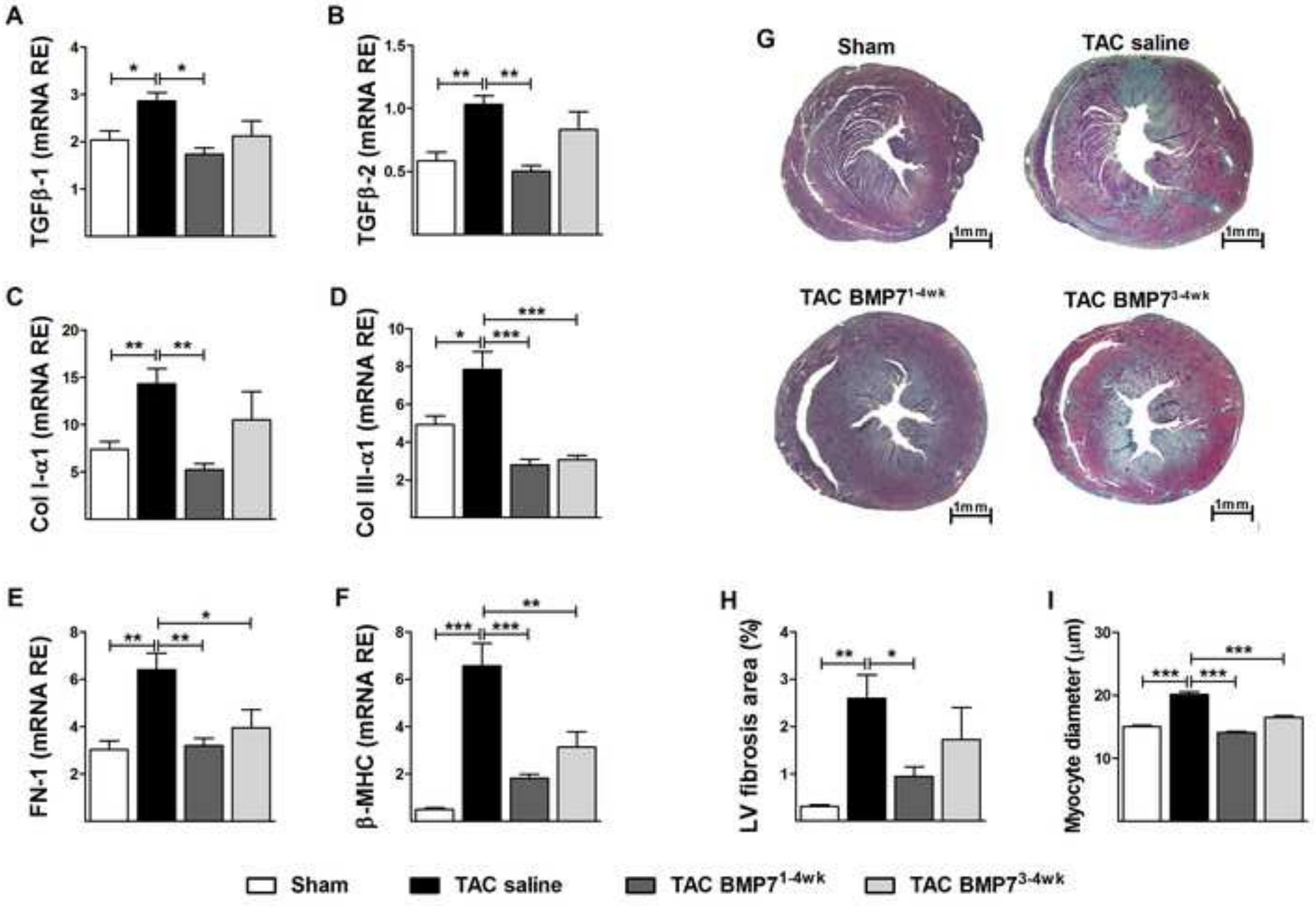

Figure 6

Click here to download Figure(s): BMP7 Fig 6 cardiovasc res.tif

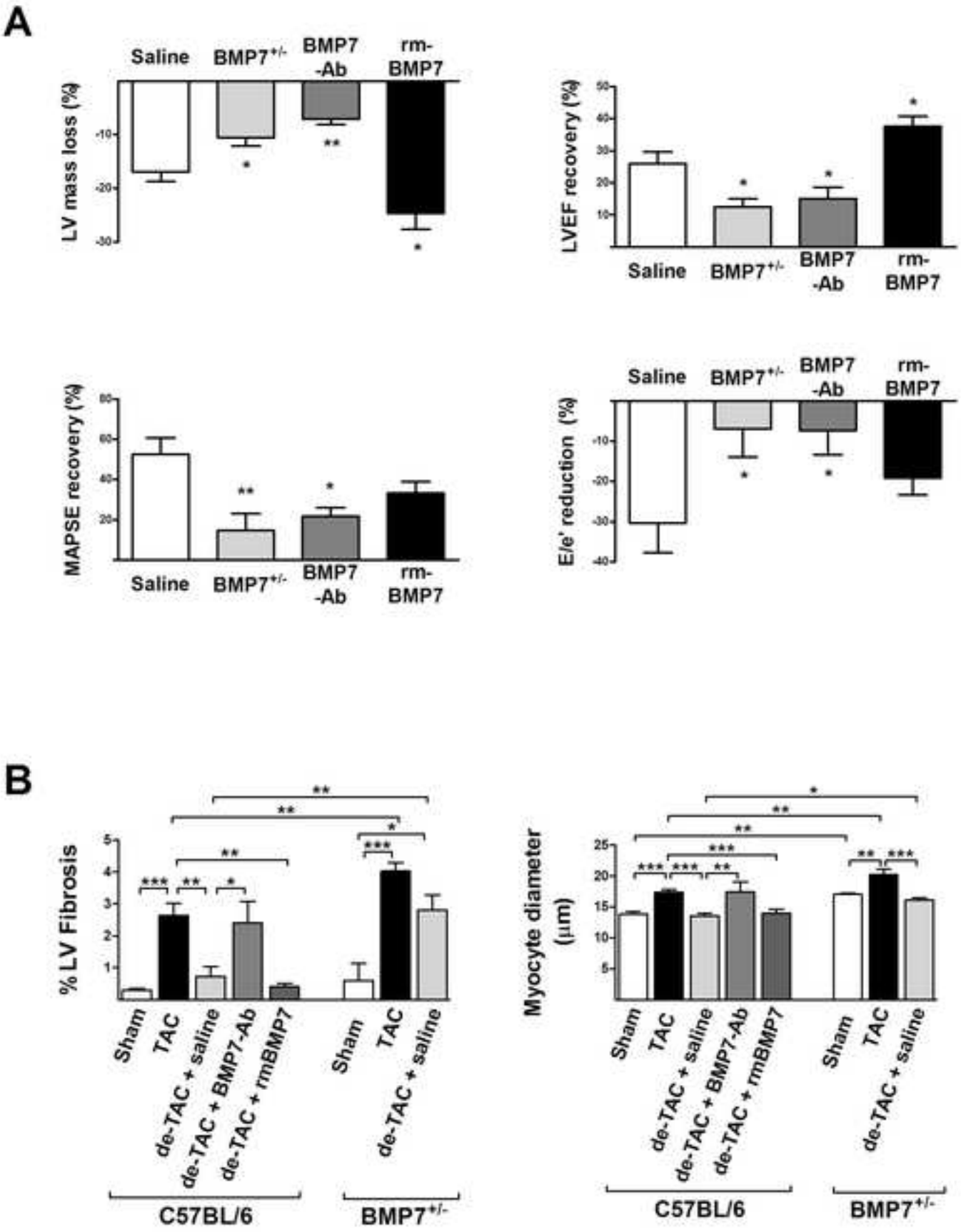

Figure 7
Click here to download Figure(s): FINAL fig 7.tif

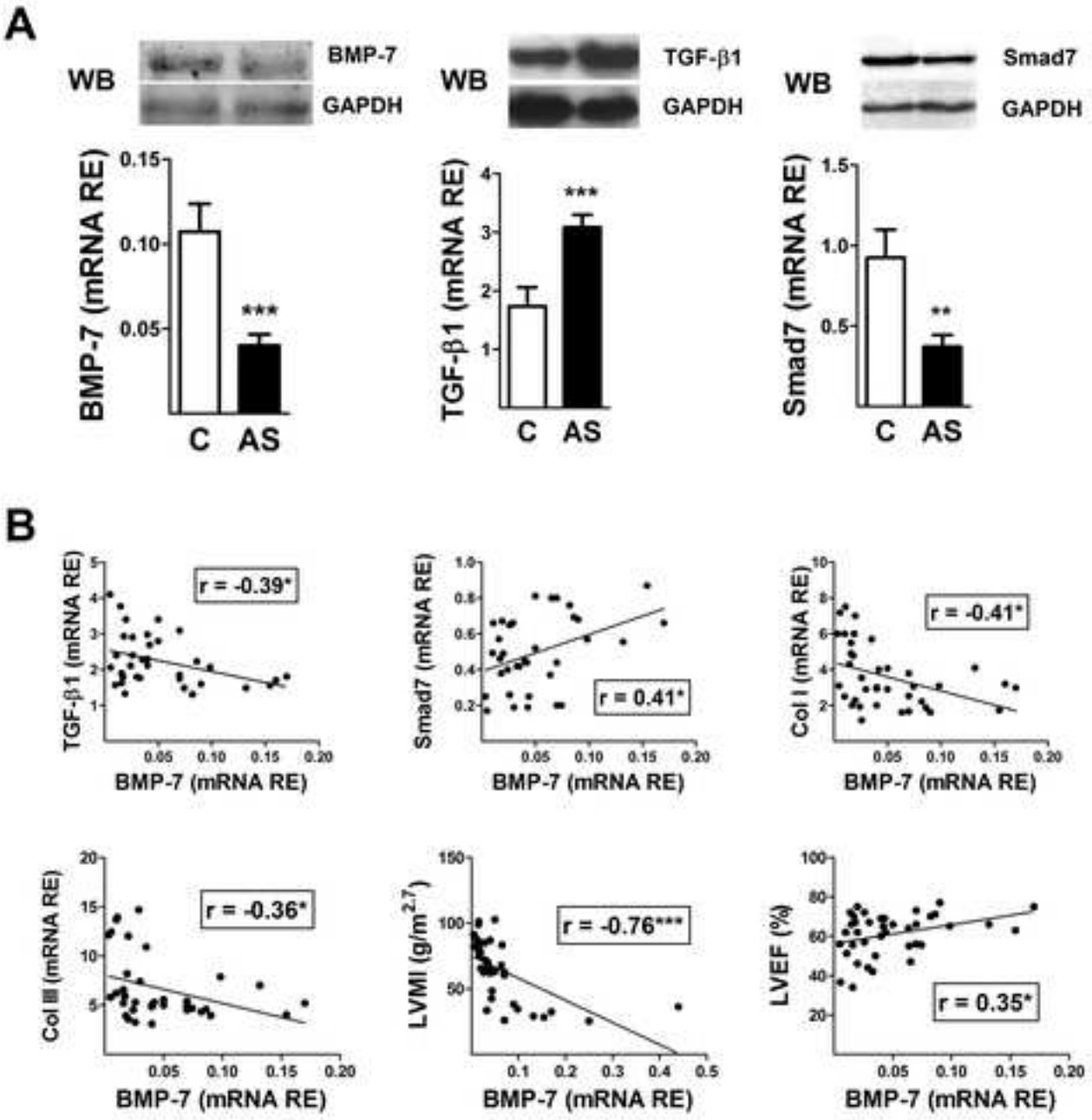

C

Predictors of LV mass (g) in AS patients *(Multiple linear regression analysis)*				
Variable	Unstandardized Coefficient		Standardized Coefficient β	p value
	B	Std. Error		
Myocardial BMP-7 (RE *vs* 18S)	-111.3	17.6	-0.72	0.0001
Myocardial TGF-β (RE *vs* 18S)	21.2	9.5	0.30	0.02

Supplementary Figure S1. Pictogram showing the protocols of treatment.

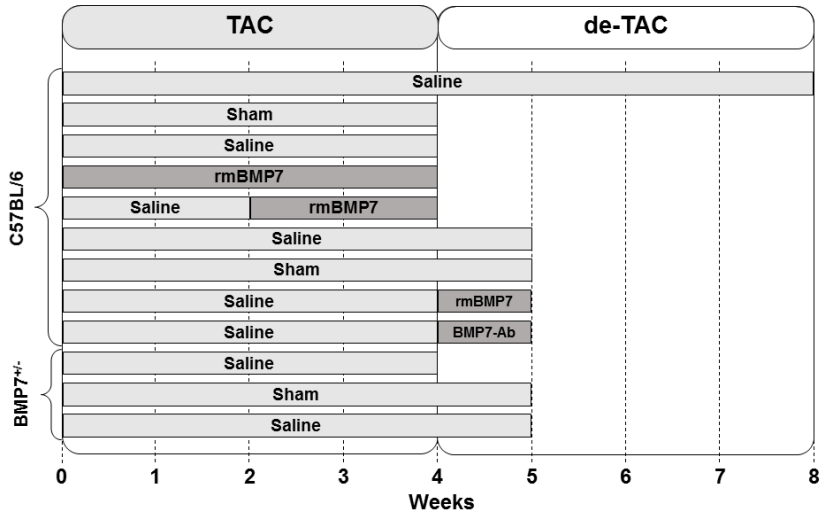

Supplementary Table1

Variable	Aortic Stenosis	Surgical Controls
n	38	32
Age (yrs ± SD)	71.2±10.1	53.6±15.5
Male/Female (n)	21/17	10/23
Systolic blood pressure, mm Hg	129.4±29.9	120.1±18.0
Diastolic blood pressure, mm Hg	67.5±10.9	69.8±10.4
Body Mass Index, kg/m^2	27.9±6.1	28.2±4.9
Systemic hypertension	52%	44%
Diabetes Mellitus	22%	6%
ACE inhibitors	24%	16%
AT-II receptor antagonists	10%	13%
Diuretics	41%	28%
Calcium antagonists	12%	3 9%
β-Blockers	28%	31%
Statins	30%	6%

ACE = Angiotensin converting enzyme; AT-II = Angiotensin II

Supplementary Statistical analysis

Figure 1.

A: Repeated-measures ANOVA followed by Bonferroni's test.
Mean trans-coarctation pressure gradient; CAT (Follow-up time: $F(4,84)=119.3$, $p<0.001$); de-CAT (Follow-up time: $F(3.30)=176.4$, $p<0.001$).
Posterior wall thickness: CAT (Follow-up time: $F(4,84)=158.9$, $p<0.001$); de-CAT (Follow-up time: $F(3,30)=54.3$, $p<0.001$).
LV mass: CAT (Follow-up time: $F(4,84)=114.8$, $p<0.001$); de-CAT (Follow-up time: $F(3,30)=45.1$, $p<0.001$).
LV end diastolic diameter: TAC (Follow-up time: $F(4,84)=3.85$, $p<0.01$).
Relative PWT to LVED radius: TAC (Follow-up time: $F(4,84)=12.2$, $p<0.001$); de-TAC (Follow-up time: $F(3,30)=11.0$, $p<0.001$).
LV ejection fraction: TAC (Follow-up time: $F(4,84)=37.4$, $p<0.001$); de-TAC (Follow-up time: $F(3,30)=36.1$, $p<0.001$).
Mitral annular plane systolic excursion: TAC (Follow-up time: $F(4,84)=31.1$, $p<0.001$); de-TAC (Follow-up time: $F(3,30)=18.8$, $p<0.001$)].
Ratio of peak early transmitral flow velocity (E) to peak early myocardial tissue velocity (e′): [TAC (Follow-up time: $F(4,40)=24.9$, $p<0.001$); de-TAC (Follow-up time: $F(3,30)=28.5$, $p<0.001$)].
B: ANOVA followed by Bonferroni's test.
BMP7: $F(2,20)=6.56$, $p<0.01$; TGF-β1: $F(2,21)=7.68$, $p<0.01$; TGF-β2: $F(2,21)=47.5$, $p<0.001$; TGF-β1/BMP-7: $F(2,20)=8.9$, $p<0.01$; TGF-β2/BMP-7: $F(2,21)=14.6$, $p<0.001$.
C: ANOVA followed by Bonferroni's test.
p-Smad 1/5/8: $F(2,12)=15.5$, $p<0.001$; p-Smad 2/3: $F(2,12)=7.6$, $p<0.05$; and Smad 7: mRNA: $F(2,18)=7.3$, $p<0.01$.

Figure 3: ANOVA followed by Bonferroni's test.
ANP: $F(2,14)=11.4$, $p<0.01$; BNP: $F(2,14)=9.7$, $p<0.01$; β-MHC: $F(2,14)=4.4$, $p<0.05$. Luciferase Activity: $F(2,13)=3.8$, $p<0.05$.

Figure 4

A: Two way repeated-measures ANOVA followed by Bonferroni's test.
LV mass: TAC-saline *vs.* TAC-BMP-$7^{1\text{-}4wk}$: (Interaction: $F(4,44)=22.9$, $p<0.001$; Follow-up time: $F(4,44)=133.7$ $p<0.001$; Treatment: $F(1,44)=27.3$, $p<0.001$); TAC-saline vs. TAC-BMP-$7^{3\text{-}4wk}$: (Interaction: $F(2,28)=6.8$, $p<0.001$; Follow-up time: $F(2,28)=4.2$, $p<0.001$; Treatment: $F(1,14)=30.0$, $p<0.05$).
Posterior wall thicknesses: TAC-saline *vs.* TAC-BMP-$7^{1\text{-}4wk}$: (Interaction: $F(4,44)=9.8$, $p<0.001$; Follow-up time: $F(4,44)=143.7$ $p<0.001$; Treatment: $F(1,44)=36.8$, $p<0.001$); TAC-saline vs. TAC-BMP-$7^{3\text{-}4wk}$: (Interaction: $F(2,28)=3.4$, $p<0.05$).
LV end systolic diameter: TAC-saline *vs*. TAC-BMP-$7^{1\text{-}4wk}$: (Interaction: $F(4,44)=15.0$, $p<0.001$; Follow-up time: $F(4,44)=16.9$ $p<0.001$; Treatment: $F(1,44)=27.9$, $p<0.001$); TAC-saline *vs*. TAC-BMP-$7^{3\text{-}4wk}$: (Interaction: $F(2,28)=3.7$, $p<0.01$; Follow-up time: $F(2,28)=4.7$, $p<0.01$; Treatment: $F(1,14)=30.7$, $p<0.05$).
LV end diastolic diameter: TAC-saline *vs*. TAC-BMP-$7^{1\text{-}4wk}$ (Interaction: $F(4,44)=16.3$, $p<0.001$; Follow-up time: $F(4,44)=15.3$ $p<0.001$; Treatment:

F(1,44)=24.2, p<0.001); TAC-saline *vs*. TAC-BMP-$7^{3\text{-}4wk}$: (Follow-up time: F(2,28)=9.5, p<0.001).
LV ejection fraction: TAC-saline *vs*. TAC-BMP-$7^{1\text{-}4wk}$: (Interaction: F(4,44)=8.1, p<0.001; Follow-up time: F(4,44)=11.7, p<0.001; Treatment: F(1,44)=21.9, p<0.001); TAC-saline *vs.* TAC-BMP-$7^{3\text{-}4wk}$: (Interaction: F(2,28)=9.5, p<0.001; Treatment: F(1,14)=27.1, p<0.05).
Mitral annular plane systolic excursion: TAC-saline *vs*. TAC-BMP-$7^{1\text{-}4wk}$: (Interaction: F(4,44)=9.4, p<0.001; Follow-up time: F(4,44)=40.0, p<0.001; Treatment: F(1,44)=13.4, p<0.01), TAC-saline *vs*. TAC-BMP-$7^{3\text{-}4wk}$: (Treatment F(1,14)=19.6, p<0.05).
Ratio of peak early transmitral flow velocity (E) to peak early myocardial tissue velocity (e′): TAC-saline *vs*. TAC-BMP-$7^{1\text{-}4wk}$: (Interaction: F(4,44)=12.1, p<0.001; Follow-up time: F(4,44)=20.2, p<0.001; Treatment: F(1,44)=50.5, p<0.001); TAC-saline *vs*. TAC-BMP-$7^{3\text{-}4wk}$: (Interaction: F(4,56)=2.6, p<0.05; Follow-up time: F(4,56)=66.5, p<0.001; Treatment: F(1,44)=50.5, p<0.001).
Mean trans-coarctation pressure gradient: TAC-saline *vs*. TAC-BMP-$7^{1\text{-}4wk}$: (Follow-up time: F(4,44)=190.2, p<0.001), TAC-saline *vs.* CAT-BMP-$7^{3\text{-}4wk}$: (Follow-up time: F(2,30)=10.5, p<0.001).
B: Two way repeated-measures ANOVA followed by Bonferroni's test. Pressure gradient: (Follow-up time: F(4,112)=205,4 p<0,001).
LV posterior wall thickness: (Follow-up time: F(4,112)=90.7, p<0.001; Genotype: F(1,112)=13.9, p<0.001).
IVS: Follow-up time: F(4,112)=195,1 p<0,001; Genotype: F(1,28)=21,8 p<0,001.
Relative PWT to LVED radius: (Follow-up time: F(4,112)=30.1, p<0.001; Genotype: F(1,112)=8.9, p<0.01).
LV ejection fraction (Follow-up time: F(4,112)=72.2, p<0.001).
Mitral annular plane systolic excursion (Follow-up time: F(4,112)=111.7, p<0.001).
Ratio of peak early transmitral flow velocity (E) to peak early myocardial tissue velocity (e′) (Follow-up time: F(4,112)=81.9, p<0.001).

Figure 5: ANOVA followed by Bonferroni's test.
TGF-β1: F(3,33)=5.2, p<0.01; TGF-β2: F(3,24)=7.9, p<0.001; Col I: F(3,29)=6.7, p<0.01; Col III: F(3,24)=12.8, p<0.001; FN1: F(3,21)=8.0, p<0.01; β-MHC: F(3,24)=16.0, p<0.001; histological fibrosis: F(3,24)=6.1, p<0.01; cardiomyocyte diameter: F(3,16)=19.8, p<0.001]

Figure 6
A: One way ANOVA followed by Bonferroni's test.
LV hypertrophy regression after de-TAC: F(3,25)=15.03, p<0.001.
Recovery of systolic function in the short axis (LVEF): F(3,24)=10.2, p<0.001.
Recovery of systolic function in the long axis (MAPSE): F(3,24)=5.5, p<0.01.
Reduction of LV loading pressure (E/e'): F(3,25)=3.0, p<0.05.
B: One way ANOVA followed by Bonferroni's test.
Histological fibrosis: F(7,40)=13.9, p<0.001; cardiomyocyte diameter: F(7,42)=14.8, p<0.01).